

Geophysical Research Letters[®]



RESEARCH LETTER

10.1029/2023GL104072

A Gradient Boosting Decision Tree Based Correction Model for AIRS Infrared Water Vapor Product

Jiafei Xu¹  and Zhizhao Liu¹ 

¹Department of Land Surveying and Geo-Informatics, Hong Kong Polytechnic University, Hung Hum, Hong Kong

Key Points:

- A Gradient Boosting Decision Tree based correction model for Atmospheric Infrared Sounder (AIRS) infrared (IR) precipitable water vapor (PWV) products is developed and validated
- The model can significantly enhance the all-weather accuracy of AIRS IR PWV products, especially in dry atmospheric conditions
- The model reduces the root-mean-squared error of AIRS IR PWV by 21.43% with GNSS PWV, by 17.28% with radiosonde PWV, and by 18.13% with ERA5 PWV

Correspondence to:

Z. Liu,
lszliu@polyu.edu.hk

Citation:

Xu, J., & Liu, Z. (2023). A Gradient boosting decision tree based correction model for AIRS infrared water vapor product. *Geophysical Research Letters*, 50, e2023GL104072. <https://doi.org/10.1029/2023GL104072>

Received 10 APR 2023

Accepted 16 JUN 2023

Author Contributions:

Conceptualization: Zhizhao Liu

Data curation: Zhizhao Liu

Formal analysis: Jiafei Xu

Funding acquisition: Zhizhao Liu

Investigation: Jiafei Xu, Zhizhao Liu

Project Administration: Zhizhao Liu

Resources: Zhizhao Liu

Software: Jiafei Xu

Supervision: Zhizhao Liu

Validation: Jiafei Xu

Writing – original draft: Jiafei Xu

Writing – review & editing: Zhizhao Liu

Abstract High-quality precipitable water vapor (PWV) measurements have an essential role in climate change and weather prediction studies. The Atmospheric Infrared Sounder (AIRS) instrument provides an opportunity to measure PWV at infrared (IR) bands twice daily with nearly global coverage. However, AIRS IR PWV products are easily affected by the presence of clouds. We propose a Gradient Boosting Decision Tree (GBDT) based correction model (GBCorM) to enhance the accuracy of PWV products from AIRS IR observations in both clear-sky and cloudy-sky conditions. The GBCorM considers many dependence factors that are in association with the AIRS IR PWV's performance. The results show that the GBCorM greatly improves the all-weather quality of AIRS IR PWV products, especially in dry atmospheric conditions. The GBCorM-estimated PWV result in the presence of clouds shows an accuracy comparable with that of official AIRS IR PWV products in clear-sky conditions, demonstrating the capability of the GBCorM model.

Plain Language Summary Water vapor is a dominant natural greenhouse gas in the atmosphere, which plays a vital role in atmospheric circulation, energy exchange, and hydrological cycle in association with climate change. The Atmospheric Infrared Sounder (AIRS) instrument, onboard the Aqua satellite platform, can provide twice per day, near-global precipitable water vapor (PWV) measurements using infrared (IR) bands. However, due to the effect of clouds, the accuracy of AIRS IR PWV products in cloudy sky conditions is often inferior to that in cloud-free sky conditions. In this study, we proposed a Gradient Boosting Decision Tree (GBDT) based correction model (GBCorM) to improve the all-weather quality of AIRS IR PWV products. We found that the GBCorM can significantly enhance the accuracy of AIRS IR PWV products in all weather conditions, especially for dry atmospheric conditions. The enhanced AIRS IR PWV data records will be more suitable for weather forecasting locally or globally as well as climate monitoring. In addition to the AIRS instrument, this GBCorM could be a promising approach to enhance the all-weather quality of IR PWV products from other satellite-born instruments.

1. Introduction

Atmospheric water vapor is a dominant natural greenhouse component in association with atmospheric circulation, energy exchange, and hydrological cycle (Colman, 2003; Myhre et al., 2013; Sherwood et al., 2010), which accounts for about 60% of the total greenhouse warming effect of the Earth (Held & Soden, 2000). Water vapor varies significantly in the spatial and temporal coverages (Trenberth et al., 2005), exerting a positive feedback in climate change (Schneider et al., 2010; Soden et al., 2002). It is also an important parameter in numerical weather prediction models (Manandhar et al., 2019; Rohm et al., 2019). Hence, proper spatial-temporal resolution water vapor observations are essential to advance the understanding of climate and weather locally or globally.

Precipitable water vapor (PWV) is a widely used measurement of the total atmospheric water vapor content contained in a vertical column of a cross-section unit (Kaufman & Gao, 1992). The ground-based radiosonde instrument has been employed to observe PWV (Ross & Elliot, 2001), which is considered a very reliable in-situ water vapor measurement technique frequently used as a reference to validate other water vapor measurements (Piesanie et al., 2013). However, the PWV measured from radiosonde has a poor time resolution with one or two observations daily, as it can be easily affected by weather conditions (Vaquero-Martínez et al., 2018). In contrast, the in-situ Global Navigation Satellite System (GNSS) instrument can provide continuous PWV observations at a high temporal resolution in all-weather conditions (Bevis et al., 1992), showing an accuracy lower than 3 mm against radiosonde-based water vapor measurements (Wang & Zhang, 2008). The GNSS PWV data have been used as a reference to test other water vapor observation approaches (Vaquero-Martínez et al., 2018; Xu & Liu, 2021b), or as input data in model construction (Bai et al., 2021; Xu & Liu, 2021a). Nevertheless,

© 2023. The Authors.

This is an open access article under the terms of the [Creative Commons Attribution-NonCommercial-NoDerivs License](https://creativecommons.org/licenses/by-nc-nd/4.0/), which permits use and distribution in any medium, provided the original work is properly cited, the use is non-commercial and no modifications or adaptations are made.

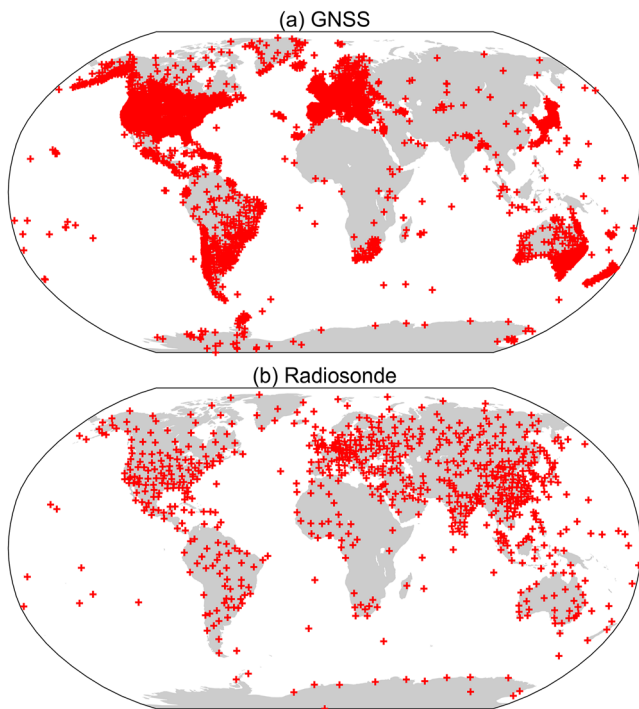


Figure 1. Geographical distribution of (a) 10,465 GNSS stations and (b) 783 radiosonde stations.

the ground-based water vapor measurement methods, that is, radiosonde and GNSS, can only provide point-wise PWV data at specific stations without global coverage.

On the other hand, satellite remote sensing techniques provide a unique opportunity to measure PWV at a reasonable spatial and temporal resolution using different spectral wavelength bands, namely visible (Wang et al., 2014), near-infrared (Gao & Kaufman, 2003), infrared (IR) (Seemann et al., 2003), and microwave (Ji et al., 2017). The Atmospheric Infrared Sounder (AIRS) sensor, onboard the Aqua satellite launched on 4 May 2002, is capable of continuously providing water vapor data products using IR observations, covering near-global coverage with a high temporal resolution twice per day (Aumann et al., 2003). The quality of AIRS IR PWV products is usually affected by the presence of clouds, as IR observations are sensitive to clouds (Vaquero-Martínez et al., 2018). In addition to clouds, other dependence parameters are also reported to affect the performance of satellite IR PWV products, such as location, PWV values, seasonality, land surface temperature, land surface types, and solar zenith angle data (Aumann et al., 2003; Vaquero-Martínez et al., 2018). In the work by Chang et al. (2020), a differential linear adjustment model (DLAM) is developed for AIRS IR PWV products based on ERA-Interim water vapor data, showing that the root-mean-squared error (RMSE) of DLAM-estimated PWV is reduced by around 16% compared with in-situ radiosonde PWV observations. The performance of the DLAM is validated by the same data sets used for model training (Chang et al., 2020). The performance of DLAM, developed using reanalysis-based PWV data, is not as good as that of models developed based on in-situ PWV measurements (Xu & Liu, 2022). To date, little study has been reported on the calibration of satellite IR PWV products by considering various dependence factors.

Here, we develop a Gradient Boosting Decision Tree (GBDT) based correction model (GBCorM) to enhance the quality of PWV products from AIRS IR measurements under all-weather conditions. The GBCorM utilizes AIRS IR PWV, latitude, longitude, month, solar zenith angle, surface skin temperature, surface class, quality flag, and cloud fraction data, which are associated with the performance of AIRS IR PWV products. In the model development procedure, the worldwide in-situ GNSS and radiosonde PWV measurements collected during 2017–2019 are employed. The validation of the GBCorM is performed using global water vapor observations collected from GNSS, radiosonde, and ERA5 in 2020.

2. Data

The AIRS sensor, onboard the Aqua satellite platform, is a modern hyperspectral IR sounder (Aumann et al., 2003). It can provide near-global PWV observations twice daily at IR channels (Aumann et al., 2003). The AIRS products utilized in this research are Aqua/AIRS L2 Standard Physical Retrieval (AIRS-only) V7.0 at GES DISC (AIRS2RET v7.0) (AIRS project, 2019). This product consists of cloud and surface parameters, as well as profiles of temperature, water vapor, ozone, carbon monoxide, and methane, with a spatial resolution of 50 km. In this paper, the total PWV data records (totH2OStd) of AIRS Standard Physical Retrieval were employed. The AIRS2RET v7.0 global data products collected during 2017–2019 were selected for GBCorM model construction and training. The one-year AIRS-based global PWV data records observed in 2020 were used to test the performance of the GBCorM. The global PWV data set includes in-situ PWV measurements from 10,465 GNSS stations as well as 783 radiosonde stations. Figure 1 shows the geographical distribution of in-situ GNSS and radiosonde stations. In addition, the reanalysis-based water vapor data records, obtained from ERA5 for the year 2020, are also used to test the performance of the GBCorM. To have a better comparison with GNSS and radiosonde results, only ERA5 PWV data at the locations of global GNSS and radiosonde stations are used in the validation. Our analysis indicates that the accuracy of ERA5 PWV data is better than 3 mm when compared

with GNSS and radiosonde PWV data. To better quality control the ERA5 PWV data used for the validation, we require the difference between ERA5 PWV and GNSS (or radiosonde) PWV be no larger than 3 mm.

The global ERA5 PWV data (Hersbach et al., 2020) from the European Centre for Medium-Range Weather Forecasts (ECMWF), were employed. The ground-based GNSS water vapor data records, provided by the Nevada Geodetic Laboratory (Blewitt et al., 2018), are estimated from GNSS wet zenith delay observations using the retrieval method developed by Bevis et al. (1994). The radiosonde measurements at both 0000 UTC and 1200 UTC daily were obtained from the Integrated Radiosonde Archive Version 2 (IGAR2) (Durre et al., 2016). The PWV retrieval from the IGAR2 radiosonde observations is based on the approach developed in Zhang et al. (2019). The GNSS and radiosonde global PWV data observed in 2017–2019 were used for model development. The performance of the GBCorM was validated based on global PWV data observed from GNSS, radiosonde, and ERA5 in 2020.

3. Method

The GBDT is a tree-based ensemble machine learning approach, which can be utilized in regression and classification problems (Friedman, 2002). It includes a number of decision trees as weak learners in order to obtain a strong decision tree learner. The decision trees of the GBDT algorithm are fitted relying upon the residual error of the former decision tree. The output from GBDT is a weighted average result from the output results of all decision trees.

We have developed a GBCorM to enhance the accuracy of AIRS IR PWV products under all-weather conditions based on in-situ PWV observations from GNSS and radiosonde instruments. The key concept in the GBCorM is to link the GNSS and radiosonde PWV to a set of AIRS IR PWV, latitude, longitude, month, solar zenith angle, surface skin temperature, surface class, quality flag, and CF data using the GBDT-based machine learning approach. These multiple variables are associated with the performance of AIRS IR PWV measurements (Aumann et al., 2003; Vaquero-Martínez et al., 2018). The GBCorM is defined as:

$$W = \text{GBDT}(W_{\text{AIRS}}, \text{LAT}, \text{LON}, \text{MON}, \text{SZA}, \text{SST}, \text{SC}, \text{QF}, \text{CF}) \quad (1)$$

where W is the in-situ GNSS and radiosonde PWV data, W_{AIRS} is the official AIR IR PWV product, LAT is the latitude with the unit of degree, LON is the longitude with the unit of degree, MON is the month number of the year, SZA is the solar zenith angle with the unit of degree, SST is the surface skin temperature with the unit of K, SC is the surface class, QF is the quality flag of official AIRS IR PWV products, and CF is the cloud fraction information. The W_{AIRS} , LAT, LON, MON, SZA, SST, SC, QF, and CF parameters can be obtained from the official AIRS2RET v7.0 data products.

In order to perform the GBCorM modeling and testing, it is important to collocate satellite-based AIRS observations with GNSS, radiosonde, and ERA5 data in the spatial and temporal domains, that is, building input–output data pairs. In this research, we require the spatial distance between AIRS with GNSS, radiosonde, or ERA5 be as small as possible, with the distance not exceeding 100 km. Temporally, the observation time difference between AIRS with GNSS or ERA5 is required to be smaller than 30 min. The AIRS–radiosonde time difference has to be smaller than 1 hr.

In the model training procedure, a total of 1,016,438 AIRS–GNSS data pairs and 16,534 AIRS–radiosonde data pairs were spatiotemporally matched in 2017–2019. The parameters of the GBCorM were optimized based on the 5-fold cross validation approach. With this 5-fold cross validation method, the training datasets were randomly divided into five groups, where four of those groups were employed for model training and the remaining one-fifth of data set was used for model testing. Then we applied the GBCorM model to correct AIRS IR global PWV products in 2020. The GBCorM-estimated AIRS IR PWV data were validated with global GNSS, radiosonde, and ERA5 PWV observations in 2020.

4. Results and Discussion

In this study, three evaluation metrics, namely coefficient of determination (R^2), RMSE, and mean bias (MB), are utilized to assess the accuracy of AIRS IR PWV observations by conducting comparisons with reference PWV observations from GNSS, radiosonde, and ERA5. They are calculated as:

$$R^2 = \frac{\left[\sum_{i=1}^N (W_o - \overline{W}_o)(W_r - \overline{W}_r) \right]^2}{\sqrt{\sum_{i=1}^N (W_o - \overline{W}_o)^2 (W_r - \overline{W}_r)^2}} \quad (2)$$

$$\text{RMSE} = \sqrt{\frac{1}{N} \sum_{i=1}^N (W_o - W_r)^2} \quad (3)$$

$$\text{MB} = \frac{1}{N} \sum_{i=1}^N (W_o - W_r) \quad (4)$$

where W_o is the PWV observations from AIRS IR, \overline{W}_o is the averaged PWV observations from AIRS IR, W_r is the reference PWV observations from GNSS, radiosonde, or ERA5, \overline{W}_r is the averaged reference PWV observations from GNSS, radiosonde, or ERA5, and N is the number of collocated AIRS–GNSS, AIRS–radiosonde, or AIRS–ERA5 data pairs used for validation.

In the validation procedure, the $\text{CF} = 0$ condition implies that the AIRS-measured IR water vapor data are retrieved under clear sky conditions, with cloud fraction equaling to 0. The $\text{CF} = (0,1]$ condition implies that the cloud fraction indicator, associated with AIRS-derived IR PWV, is larger than 0 but not larger than 1. It suggests that the AIRS/Aqua IR water vapor products are measured in the existence of clouds, as the cloud fraction indicator is not equal to 0. The $\text{CF} = [0,1]$ condition shows that the Aqua AIRS-retrieved IR water vapor products are observed under all weather conditions including both clear-sky (i.e., $\text{CF} = 0$) and cloudy-sky (i.e., $\text{CF} = (0,1]$) conditions.

Figure 2 shows the evaluation result between AIRS IR PWV and reference PWV from GNSS, radiosonde, and ERA5 in 2020. In clear sky conditions ($\text{CF} = 0$), the correlation R^2 of GBCorM-based AIRS IR PWV estimates was enhanced to 0.92 with respect to GNSS PWV, 0.93 with respect to radiosonde PWV, and 0.93 with respect to ERA5 PWV, which were better than the official AIRS IR PWV products ($R^2 = 0.89$, $R^2 = 0.92$, and $R^2 = 0.92$). Their RMSE has reduced by 26.16% from 3.02 to 2.23 mm for GNSS PWV comparison, 17.00% from 2.47 to 2.05 mm for radiosonde PWV comparison, and 19.12% from 2.51 to 2.03 mm for ERA5 PWV comparison. The MB values were corrected to nearly 0 ($\text{MB} = 0.01$ mm, $\text{MB} = -0.00$ mm, and $\text{MB} = -0.36$ mm).

In the presence of clouds, that is, $\text{CF} = (0,1]$, the GBCorM-estimated AIRS IR PWV data had a better agreement with reference PWV from GNSS, radiosonde, and ERA5 measurements. The RMSE was reduced by 21.08% from 4.27 to 3.37 mm when compared with GNSS PWV, 17.03% from 3.64 to 3.02 mm when compared with radiosonde PWV, and 18.00% from 3.50 to 2.87 mm when compared with ERA5 PWV. The R^2 and MB were 0.92 and -0.12 mm when compared with GNSS PWV, 0.91 and -0.09 mm when compared with radiosonde PWV, and 0.93 and -0.12 mm when compared with ERA5 PWV. After the calibration by the GBCorM model, the PWV accuracy in the presence of clouds was comparable with that of official AIRS IR PWV products in clear-sky conditions. This clearly illustrates the effectiveness of the GBCorM model.

In all-weather conditions ($\text{CF} = [0,1]$), taking the GNSS PWV as reference, the GBCorM-based AIRS IR PWV data showed a reduction in RMSE by 21.43% from 4.17 to 3.28 mm, with an increase in R^2 from 0.90 to 0.92 and a reduction in MB reduced from 0.39 to -0.11 mm. When compared with radiosonde PWV observations, the GBCorM-estimated AIRS IR PWV result also showed an improved performance. The R^2 was increased from 0.90 to 0.91, RMSE was reduced 17.28% from 3.53 to 2.92 mm, and MB was reduced from -0.83 to -0.08 mm. The RMSE between PWV from AIRS IR and ERA5 was reduced by 18.13% from 3.42 to 2.80 mm, with an improvement in R^2 from 0.92 to 0.94 and a reduction in MB from 0.15 to -0.10 mm.

In terms of RMSE reduction, the GBCorM showed a larger accuracy improvement on AIRS IR PWV measurements compared with the DLAM developed in the recent work conducted by Chang et al. (2020). This can be

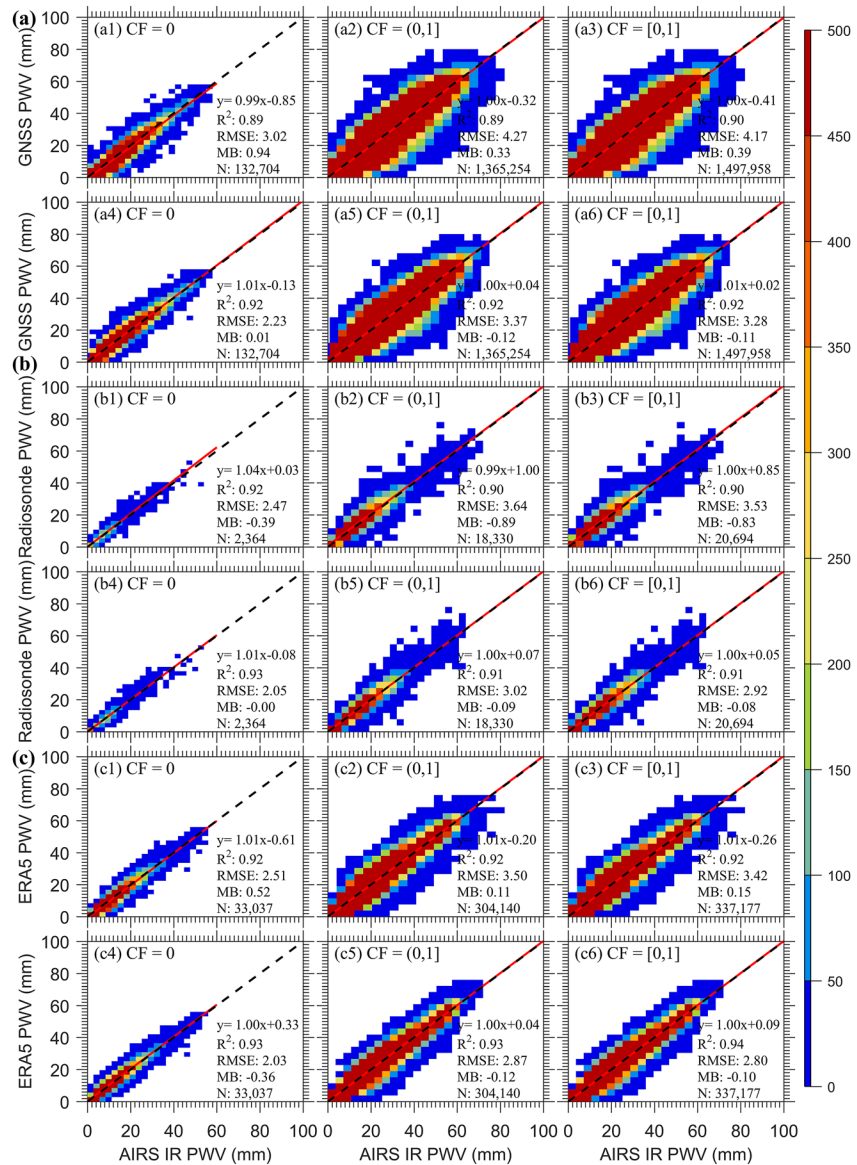


Figure 2. Comparison of satellite-based AIRS IR PWV measurements with reference PWV measurements from (a) GNSS, (b) radiosonde, and (c) ERA5 worldwide in 2020, under cloud fraction CF = 0, CF = [0, 1], CF = [0, 1] conditions. In (a) to (c), the top row uses original AIRS IR PWV products that have not been calibrated by the GBCorM model; and the bottom row uses the new AIRS IR PWV that have been calibrated by the GBCorM model. The color bar shows the size of paired data points.

explained by two reasons: (a) our GBCorM model has considered various dependence parameters that are associated with the performance of AIRS IR PWV observations and can impact the accuracy of the AIRS IR PWV data, while the DLAM did not do so; (b) the GBCorM is developed based on in-situ high-quality PWV measurements while the DLAM was developed using the reanalysis-based PWV data.

In Figure 3a, at different CF levels (CF = 0, CF = [0,1], and CF = [0,1]), the station-wise RMSE of GBCorM-based PWV result was found at most stations to be smaller than that of official AIRS IR PWV products, when compared with ground-based GNSS PWV observations. The performance of satellite-based IR PWV observations are easily affected in dry atmospheric conditions (Liu et al., 2017). After employing the GBCorM, the GNSS stations in high-latitude regions with dry atmospheric conditions tended to have larger station-wise RMSE reduction and higher accuracy improvement (see Figure 3a). This implies that the GBCorM can significantly improve the performance of AIRS IR PWV observations, especially in dry atmospheric conditions.

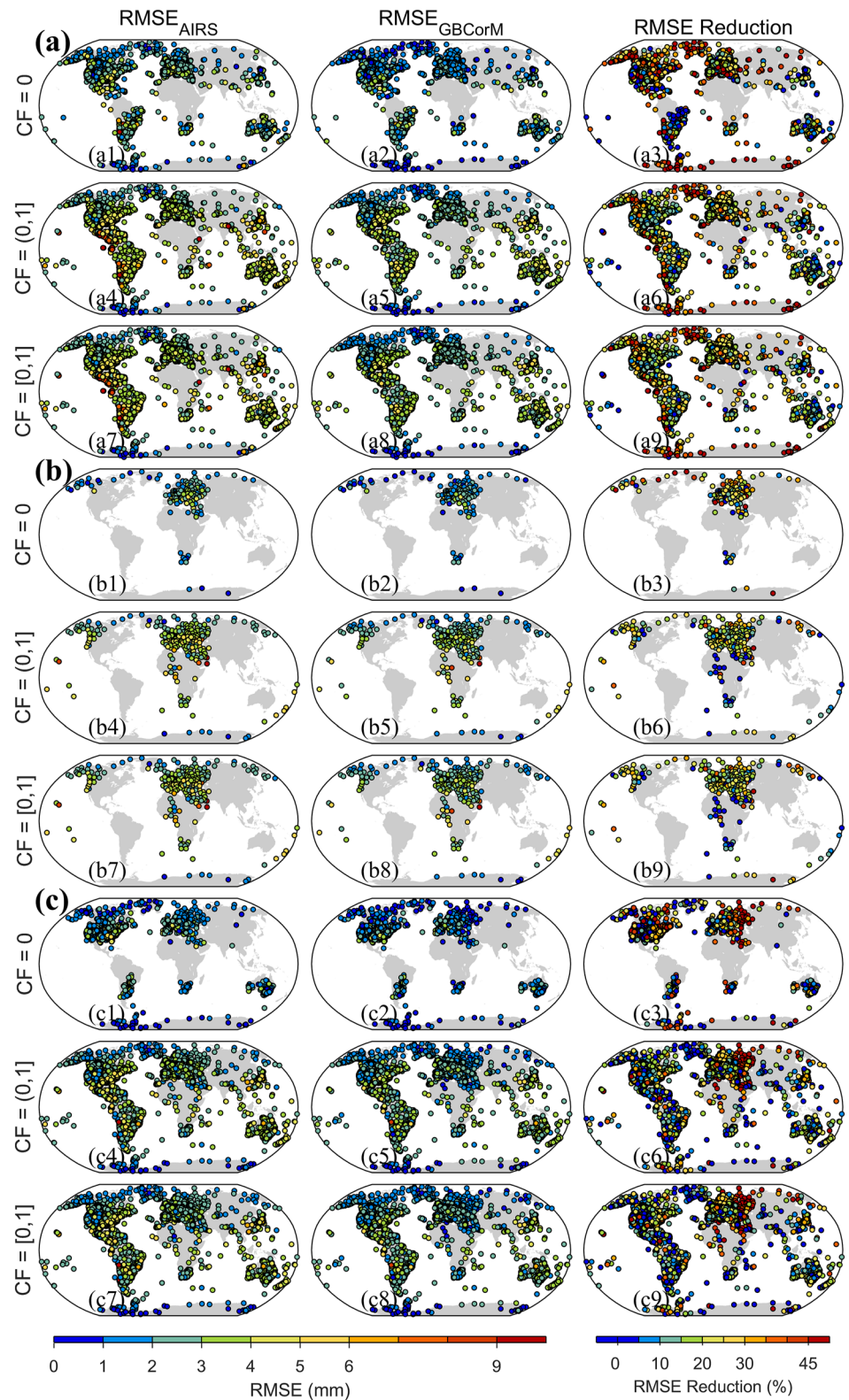


Figure 3. Station-wise comparison of satellite-based AIRS IR PWV measurements with reference PWV measurements from (a) GNSS, (b) radiosonde, and (c) ERA5 worldwide in 2020, under cloud fraction $CF = 0$, $CF = [0, 1]$, $CF = [0, 1]$ conditions. In (a) to (c), the left column shows the station-wise RMSE of AIRS IR PWV, the middle column shows the station-wise RMSE of the new AIRS IR PWV calibrated by the GBCorM model, and the right column shows the station-wise percentage of RMSE reduction between the AIRS IR PWV and the new AIRS IR PWV calibrated by the GBCorM model.

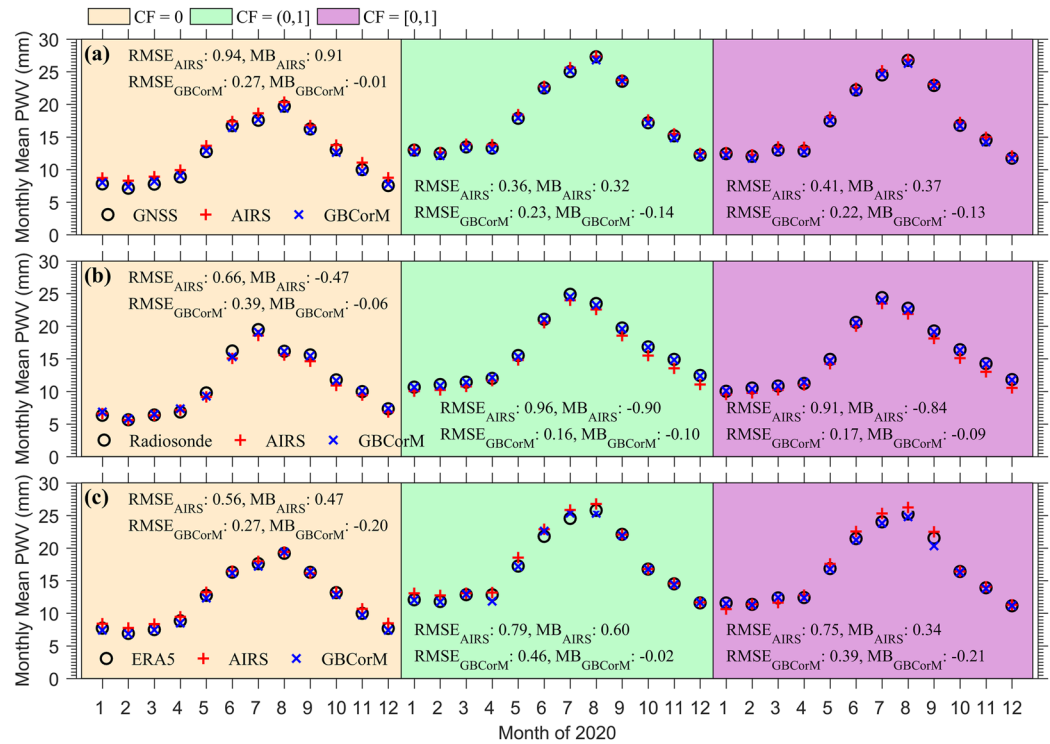


Figure 4. Comparison of monthly average PWV from satellite-based AIRS IR PWV measurements with reference PWV measurements from (a) GNSS, (b) radiosonde, and (c) ERA5 worldwide in 2020, under cloud fraction $CF = 0$, $CF = [0, 1]$, $CF = [0, 1]$ conditions.

Figure 3b also shows that the GBCorM-estimated PWV result had smaller RMSE and improved the accuracy at most radiosonde stations under $CF = 0$, $CF = [0, 1]$, and $CF = [0, 1]$ conditions. The station-wise RMSE values between GBCorM-estimated PWV and ERA5 PWV were generally lower than the official AIRS IR PWV product at most stations under $CF = 0$, $CF = [0, 1]$, and $CF = [0, 1]$ levels, illustrating an improved performance (see Figure 3c).

Figure 4 shows the comparison of monthly average PWV from GNSS, radiosonde, ERA5, AIRS IR, and GBCorM-calibrated result under $CF = 0$, $CF = [0, 1]$, and $CF = [0, 1]$ conditions. Compared with GNSS-observed reference PWV, the GBCorM-calibrated PWV result presented a monthly RMSE of 0.27 mm under $CF = 0$, 0.23 mm under $CF = [0, 1]$, and 0.22 mm under $CF = [0, 1]$, better than the official AIRS-observed IR water vapor product (RMSE = 0.94, 0.36, and 0.41 mm, respectively). The monthly RMSE between PWV from AIRS and radiosonde instruments reduced from 0.66 to 0.39 mm, from 0.96 to 0.16 mm, and from 0.91 to 0.17 mm under $CF = 0$, $CF = [0, 1]$, and $CF = [0, 1]$ conditions, respectively. The monthly MB values were close to 0 after calibration by the GBCorM method. The GBCorM-estimated monthly mean PWV had a better agreement with reference ERA5 PWV than the official AIRS IR water vapor estimates. In general, the GBCorM-estimated PWV has a better agreement with the reference PWV (i.e., GNSS, radiosonde, or ERA5) in most months of 2020 under different cloud fraction levels (different CF values).

5. Conclusions

A GBCorM model is for the first time developed to improve the accuracy of PWV products under all-weather conditions from AIRS IR observations. The GBCorM model considers AIRS IR PWV, latitude, longitude, month, solar zenith angle, surface skin temperature, surface class, quality flag, and cloud fraction factors, which can affect the accuracy of AIRS IR PWV products. The ground-based global GNSS and radiosonde PWV data observed during 2017–2019 are employed for the construction and training of the GBCorM. The global PWV data from GNSS, radiosonde, and ERA5 in 2020 are utilized for validation process.

The GBCorM-based PWV estimates agree better with reference PWV observations from GNSS, radiosonde, and ERA5. Under CF = 0 (cloud-free sky) condition, their correlation R^2 are found to be 0.92 with GNSS PWV, 0.93 with radiosonde PWV, and 0.93 with ERA5 PWV, which are higher than official AIRS IR PWV products ($R^2 = 0.89$, $R^2 = 0.92$, and $R^2 = 0.92$). The RMSE is reduced by 26.16% from 3.02 to 2.23 mm (GNSS PWV), by 17.00% from 2.47 to 2.05 mm (radiosonde PWV), and by 19.12% from 2.51 to 2.03 mm (ERA5 PWV). In the presence of clouds (CF = [0,1]), the GBCorM-estimated PWV result shows an R^2 , RMSE, and MB of 0.92, 3.37, and -0.12 mm with respect to GNSS PWV, 0.91, 3.02, and -0.09 mm with respect to radiosonde PWV, and 0.93, 2.87, and -0.12 mm with respect to ERA5 PWV. The GBCorM model reduces the RMSE of AIRS IR PWV by 21.08% from 4.27 to 3.37 mm when evaluated by GNSS PWV, by 17.03% from 3.64 to 3.02 mm when evaluated by radiosonde PWV, and by 18.00% from 3.50 to 2.87 mm when evaluated by ERA5 PWV. The GBCorM-estimated PWV result at CF = [0,1] level was comparable with official AIRS IR PWV products at CF = 0 level, showing the effectiveness of the GBCorM.

In all-weather conditions, namely CF = [0,1], the RMSE of AIRS IR PWV after calibration by the GBCorM model is reduced by 21.43% from 4.17 to 3.28 mm when evaluated by GNSS PWV, by 17.28% from 3.53 to 2.92 mm when evaluated by radiosonde PWV, and by 18.13% from 3.42 to 2.80 mm when evaluated by ERA5 PWV. The MB of official AIRS IR PWV products is reduced from 0.39 to -0.11 mm, from 0.83 to -0.08 mm, and from 0.15 to -0.10 mm after the calibration by the GBCorM model, when evaluated by GNSS, radiosonde, and ERA5 PWV, respectively. In high-latitude regions with dry atmospheric conditions, the GBCorM-based PWV estimates show larger station-wise RMSE reduction at all CF levels (CF = 0, [0,1], and [0,1]), which implies that the GBCorM can enhance the all-weather accuracy of AIRS IR PWV products, especially in dry atmospheric conditions. The monthly average PWV result from the GBCorM model shows a better consistency with GNSS, radiosonde, and ERA5 reference PWV in most months of the year of 2020.

The improved AIRS-based water vapor data records offer a more valuable data source for climate and weather studies compared to the official AIRS PWV measurements. Additionally, the enhanced AIRS PWV estimates could be more advantageous to be employed in numerical weather prediction than ERA5 PWV. The AIRS-based PWV data have a much smaller latency than the ERA5 PWV data and they are more suitable for weather forecasting service. It should be mentioned that the collocated training data observations are much less in the oceanic region than in the land area, as very few GNSS and radiosonde stations are deployed in the ocean worldwide.

Data Availability Statement

All Aqua/AIRS L2 Standard Physical Retrieval (AIRS-only) V7.0 at GES DISC (AIRS2RET v7.0) data used for algorithm training and testing in the study are openly available and were acquired from the National Aeronautics and Space Administration website at https://airs12.gesdisc.eosdis.nasa.gov/opensap/hyrax/Aqua_AIRS_Level2/AIRS2RET.7.0/ (AIRS project, 2019). All GNSS data used for algorithm training and testing in the study are openly available and were acquired from the Nevada Geodetic Laboratory website at http://geodesy.unr.edu/gps_timeseries/trop/ (Blewitt et al., 2018). All radiosonde data used for algorithm training and testing in the study are openly available and were acquired from the Integrated Radiosonde Archive Version 2 (IGAR2) website at <https://www1.ncdc.noaa.gov/pub/data/igra/derived/derived-por/> (Durre et al., 2016). All ERA5 water vapor data used for algorithm testing in the study are openly available at <https://cds.climate.copernicus.eu/cdsapp#!/dataset/reanalysis-era5-single-levels?tab=form> (Hersbach et al., 2020).

References

- AIRS project. (2019). *Aqua/AIRS L2 standard physical retrieval (AIRS-only) V7.0*. Goddard Earth Sciences Data and Information Services Center (GES DISC). <https://doi.org/10.5067/VP1M6OG1X7M1>
- Aumann, H. H., Chahine, M. T., Gautier, C., Goldberg, M. D., Kalnay, E., McMillin, L. M., et al. (2003). AIRS/AMSU/HSB on the Aqua mission: Design, science objectives, data products, and processing systems. *IEEE Transactions on Geoscience and Remote Sensing*, 41(2), 253–264. <https://doi.org/10.1109/TGRS.2002.808356>
- Bai, J., Lou, Y., Zhang, W., Zhou, Y., Zhang, Z., & Shi, C. (2021). Assessment and calibration of MODIS precipitable water vapor products based on GPS network over China. *Atmospheric Research*, 254, 105504. <https://doi.org/10.1016/j.atmosres.2021.105504>
- Bevis, M., Businger, S., Chiswell, S., Herring, T., Anthes, R., Rocken, C., & Ware, R. (1994). Gps meteorology - Mapping zenith wet delays onto precipitable water. *Journal of Applied Meteorology*, 33(3), 379–386. [https://doi.org/10.1175/1520-0450\(1994\)033<0379:GMMZWD>2.0.CO;2](https://doi.org/10.1175/1520-0450(1994)033<0379:GMMZWD>2.0.CO;2)
- Bevis, M., Businger, S., Herring, T. A., Rocken, C., Anthes, R. A., & Ware, R. H. (1992). GPS meteorology: Remote sensing of atmospheric water vapor using the global positioning system. *Journal of Geophysical Research*, 97(D14), 15787–15801. <https://doi.org/10.1029/92JD01517>

Acknowledgments

The work described in this paper was partially supported by the grants from the Research Grants Council of the Hong Kong Special Administrative Region, China (Project No. PolyU/RGC 15221620/B-Q80Q and PolyU/RGC 15211919/B-Q73B). The support by the Hong Kong Polytechnic University under Grant 1-ZVVC-ZVN6 is also acknowledged. The authors would like to thank the National Aeronautics and Space Administration (NASA) Goddard Earth Sciences (GES) Data and Information Services Center (DISC) for providing AIRS data, the Nevada Geodetic Laboratory for providing GNSS data, and the Integrated Global Radiosonde Archive Version 2 (IGRA2) for providing radiosonde data.

- Blewitt, G., Hammond, W. C., & Kreemer, C. (2018). Harnessing the GPS data explosion for interdisciplinary science. *Eos*, 99, 485. <https://doi.org/10.1029/2018eo104623>
- Chang, L., Li, Y., Han, Z., Feng, G., Li, Y., & Zhang, Y. (2020). Improvement of precipitable water vapour and water vapour mixing ratio profile in atmospheric infrared sounder retrievals: Differential linear adjustment model. *International Journal of Remote Sensing*, 41(17), 6858–6875. <https://doi.org/10.1080/01431161.2020.1750736>
- Colman, R. (2003). A comparison of climate feedbacks in general circulation models. *Climate Dynamics*, 20(7), 865–873. <https://doi.org/10.1007/s00382-003-0310-z>
- Durre, I., Xungang, Y., Vose, R. S., Applequist, S., & Arnfield, J. (2016). *Integrated global radiosonde archive (IGRA) Version 2* (Vol. 10). NOAA National Centers for Environmental Information. V5X63X0Q.
- Friedman, J. H. (2002). Stochastic gradient boosting. *Computational Statistics & Data Analysis*, 38(4), 367–378. [https://doi.org/10.1016/S0167-9473\(01\)00065-2](https://doi.org/10.1016/S0167-9473(01)00065-2)
- Gao, B.-C., & Kaufman, Y. J. (2003). Water vapor retrievals using Moderate Resolution Imaging Spectroradiometer (MODIS) near-infrared channels. *Journal of Geophysical Research*, 108(D13), 4389. <https://doi.org/10.1029/2002JD003023>
- Held, I. M., & Soden, B. J. (2000). Water vapor feedback and global warming. *Annual Review of Energy and the Environment*, 25(1), 441–475. <https://doi.org/10.1146/annurev.energy.25.1.441>
- Hersbach, H., Bell, B., Berrisford, P., Hirahara, S., Horanyi, A., Muñoz-Sabater, J., et al. (2020). The ERA5 global reanalysis. *Quarterly Journal of the Royal Meteorological Society*, 146(730), 1999–2049. <https://doi.org/10.1002/qj.3803>
- Ji, D., Shi, J., Xiong, C., Wang, T., & Zhang, Y. (2017). A total precipitable water retrieval method over land using the combination of passive microwave and optical remote sensing. *Remote Sensing of Environment*, 191, 313–327. <https://doi.org/10.1016/j.rse.2017.01.028>
- Kaufman, Y. J., & Gao, B.-C. (1992). Remote sensing of water vapor in the near IR from EOS/MODIS. *IEEE Transactions on Geoscience and Remote Sensing*, 30(5), 871–884. <https://doi.org/10.1109/36.175321>
- Liu, H., Tang, S., Hu, J., Zhang, S., & Deng, X. (2017). An improved physical split-window algorithm for precipitable water vapor retrieval exploiting the water vapor channel observations. *Remote Sensing of Environment*, 194, 366–378. <https://doi.org/10.1016/j.rse.2017.03.031>
- Manandhar, S., Dev, S., Lee, Y. H., Meng, Y. S., & Winkler, S. (2019). A data-driven approach for accurate rainfall prediction. *IEEE Transactions on Geoscience and Remote Sensing*, 57(11), 9323–9331. <https://doi.org/10.1109/TGRS.2019.2926110>
- Myhre, G., Shindell, D., Bréon, F.-M., Collins, W., Fuglestedt, J., Huang, J., et al. (2013). Anthropogenic and natural radiative forcing. In *Climate change 2013: The physical science basis. Contribution of working Group I to the fifth assessment report of the intergovernmental panel on climate change* (pp. 659–740).
- du Piesanie, A., PETERS, A. J. M., Aben, I., Schrijver, H., Wang, P., & Noël, S. (2013). Validation of two independent retrievals of SCIAMACHY water vapour columns using radiosonde data. *Atmospheric Measurement Techniques*, 6(10), 2925–2940. <https://doi.org/10.5194/amt-6-2925-2013>
- Rohm, W., Guzikowski, J., Wilgan, K., & Kryza, M. (2019). 4DVAR assimilation of GNSS zenith path delays and precipitable water into a numerical weather prediction model WRF. *Atmospheric Measurement Techniques*, 12(1), 345–361. <https://doi.org/10.5194/amt-12-345-2019>
- Ross, R. J., & Elliot, W. P. (2001). Radiosonde-based Northern Hemisphere tropospheric water vapor trends. *Journal of Climate*, 14(7), 1602–1612. [https://doi.org/10.1175/1520-0442\(2001\)014<1602:RBNHTW>2.0.CO;2](https://doi.org/10.1175/1520-0442(2001)014<1602:RBNHTW>2.0.CO;2)
- Schneider, T., O’Gorman, P. A., & Levine, X. J. (2010). Water vapor and the dynamics of climate changes. *Reviews of Geophysics*, 48(3), RG3001. <https://doi.org/10.1029/2009RG000302>
- Seemann, S. W., Li, J., Menzel, W. P., & Gumley, L. E. (2003). Operational retrieval of atmospheric temperature, moisture, and ozone from MODIS infrared radiances. *Journal of Applied Meteorology and Climatology*, 42(8), 1072–1091. [https://doi.org/10.1175/1520-0450\(2003\)042<1072:OROATM>2.0.CO;2](https://doi.org/10.1175/1520-0450(2003)042<1072:OROATM>2.0.CO;2)
- Sherwood, S. C., Roca, R., Weckwerth, T. M., & Andronova, N. G. (2010). Tropospheric water vapor, convection, and climate. *Reviews of Geophysics*, 48(2), RG2001. <https://doi.org/10.1029/2009RG000301>
- Soden, B. J., Wetherald, R. T., Stenchikov, G. L., & Robock, A. (2002). Global cooling after the eruption of Mount Pinatubo: A test of climate feedback by water vapor. *Science*, 296(5568), 727–730. <https://doi.org/10.1126/science.296.5568.727>
- Trenberth, K. E., Fasullo, J., & Smith, L. (2005). Trends and variability in column-integrated atmospheric water vapor. *Climate Dynamics*, 24(7–8), 741–758. <https://doi.org/10.1007/s00382-005-0017-4>
- Vaquero-Martínez, J., Antón, M., de Galisteo, J. P. O., Cachorro, V. E., Álvarez-Zapatero, P., Román, R., et al. (2018). Inter-comparison of integrated water vapor from satellite instruments using reference GPS data at the Iberian Peninsula. *Remote Sensing of Environment*, 204, 729–740. <https://doi.org/10.1016/j.rse.2017.09.028>
- Wang, H., Liu, X., Chance, K., González Abad, G., & Chan Miller, C. (2014). Water vapor retrieval from OMI visible spectra. *Atmospheric Measurement Techniques*, 7(6), 1901–1913. <https://doi.org/10.5194/amt-7-1901-2014>
- Wang, J., & Zhang, L. (2008). Systematic errors in global radiosonde precipitable water data from comparisons with ground-based GPS measurements. *Journal of Climate*, 21(10), 2218–2238. <https://doi.org/10.1175/2007JCLI1944.1>
- Xu, J., & Liu, Z. (2021a). The first validation of Sentinel-3 OLCI integrated water vapor products using reference GPS data in Mainland China. *IEEE Transactions on Geoscience and Remote Sensing*, 60, 1–17. <https://doi.org/10.1109/TGRS.2021.3099168>
- Xu, J., & Liu, Z. (2021b). Radiance-based retrieval of total water vapor content from sentinel-3A OLCI NIR channels using ground-based GPS measurements. *International Journal of Applied Earth Observation and Geoinformation*, 104, 102586. <https://doi.org/10.1016/j.jag.2021.102586>
- Xu, J., & Liu, Z. (2022). A Linear regression of differential PWV calibration model to improve the accuracy of MODIS NIR all-weather PWV products based on ground-based GPS PWV data. *Ieee Journal of Selected Topics in Applied Earth Observations and Remote Sensing*, 15, 1–24. <https://doi.org/10.1109/JSTARS.2022.3204823>
- Zhang, Y., Cai, C., Chen, B., & Dai, W. (2019). Consistency evaluation of precipitable water vapor derived from ERA5, ERA-Interim, GNSS, and radiosondes over China. *Radio Science*, 54(7), 561–571. <https://doi.org/10.1029/2018RS006789>